PHYSICAL REVIEW B VOLUME 23, NUMBER 12 15 JUNE 1981

Theory of phonon-assisted Auger recombination in semiconductors

Masumi Takeshima
Semiconductor Research Laboratory, Matsushita Electronics Corporation, Takatsuki, Osaka, Japan
(Received 5 January 1981)

A theory is developed of phonon-assisted Auger recombination in semiconductors on the basis of the Green's-function formalism. As a result, the divergence difficulty, which is inherent in the earlier theory based on the second-order perturbation approach, can be avoided. It is shown that results of the present theory are different from those of the earlier theory in the following respects. For p-GaAs and p-GaSb the pure collision Auger recombination is almost negligible in comparison with the phonon-assisted Auger recombination over the whole temperature range of interest. The result that the pure collision Auger process is negligible even at 300 K for p-GaAs is remarkably contrasted from that of the earlier theory. The theory is applicable to p-GaSb, to which the earlier theory is not applicable. When one takes into account the free-carrier screening of the electron-phonon interaction for the first time, it is indicated that the effect is considerably important in p-GaSb but not in p-GaAs.

I. INTRODUCTION

The Auger recombination lifetime of the minority carriers is one of the key material parameters affecting the performance of many semiconductor devices, especially at high-doping levels. A number of theoretical and experimental investigations[1] have been made on the basis of the pure collision Auger process. However, with the pure collision Auger process it is insufficient to explain the recombination rate especially at low temperatures[2-5] and/or in highly doped materials.[6] To give a better explanation the phonon-assisted Auger recombination[4,7-10] and the impurity-assisted Auger recombination[11] have been proposed. The former and the latter processes have been shown to be predominant especially at low temperatures in moderately doped materials and in highly doped materials, respectively.

In the earlier theory of the phonon-assisted Auger recombination, the phonon scattering was taken into account in terms of the second-order perturbation treatment with respect to the electron-phonon interaction as well as the electron-electron interaction. Since the energy denominator involved in the theory can be zero, a divergence difficulty arose. The difficulty was avoided by making the approximation that the energy denominator is replaced by the value evaluated at the threshold of the Auger process. The approximation is valid under the condition that for a direct-gap semiconductor the value of the band-gap energy E_G minus the spin split-off energy Δ_0 is sufficiently larger than the thermal energy T. Therefore the theory is not applicable to the high-temperature case and/or to such materials with E_G close to Δ_0 as GaSb and InAs.

The present paper describes a theory of the minority-carrier lifetime of the phonon-assisted Auger recombination based on the Green's-function formalism. There appears no divergence difficulty, so that the present theory is applicable to any semiconductors at arbitrary temperatures. The free-carrier screening of the electron-phonon interaction is taken into account. However, we do not consider the effect of the electron-impurity interaction, which is important at high doping levels,[11] i.e., for impurity concentrations exceeding about 10^{19} cm^{-3}. Investigation of the combined effects of the phonon scattering and the impurity scattering on the Auger process will be presented in the future.

II. MODEL AND BASIC FORMULATION

In this section the minority-carrier lifetime of the phonon-assisted Auger recombination is expressed in terms of the Green's function. First we define our model by writing down the Hamiltonian as

$$H=H_E+H_P+H_{EP}+H_{EE}. \tag{2.1}$$

Here H_E, H_P, H_{EP}, and H_{EE} are the Hamiltonians for the band electrons, the phonons, the electron-phonon interaction, and the electron-electron Coulomb interaction. We assume H_E+H_P and $H_{EP}+H_{EE}$ to be the unperturbed Hamiltonian and the perturbation, respectively. The explicit forms of the Hamiltonians are

$$H_E=\sum_{l\vec{k}\sigma}\xi_l(\vec{k})a^\dagger_{l\vec{k}\sigma}a_{l\vec{k}\sigma}, \tag{2.2}$$

$$H_P=\sum_{\nu\vec{q}}\omega_\nu(\vec{q})b^\dagger_{\nu\vec{q}}b_{\nu\vec{q}}, \tag{2.3}$$

$$H_{EP}=\frac{1}{\sqrt{V}}\sum_{\nu\vec{q}\,l\vec{k}\sigma}g_\nu(\vec{q})(b^\dagger_{\nu\vec{q}}+b_{\nu\vec{q}})a^\dagger_{l\vec{k}+\vec{q}\sigma}a_{l\vec{k}\sigma}, \tag{2.4}$$

TABLE I. The list of $|g_\nu(\vec{q})|^2$.

Scattering mode	$\lvert g_\nu(\vec{q})\rvert^2$
Piezoelectric scattering (PE)	$\frac{e^2P_{PE}^2\omega_{AC}(\vec{q})}{2q^2}$
Acoustic deformation potential scattering (AC)	$\frac{\Xi^2\omega_{AC}(\vec{q})}{2c_l}$
Nonpolar optical deformation potential scattering (NPO)	$\frac{E_{NPO}^2\omega_{OP}(\vec{q})}{2\bar{c}}$
Polar optical phonon scattering (PO)	$\frac{2\pi e^2\omega_{OP}(\vec{q})}{\epsilon^* q^2}$

$$H_{EE}=\frac{1}{2V}\sum_{\substack{l_1l_2l_3l_4\\ \vec{k}\vec{k}'\vec{q}\sigma\sigma'}} v(\vec{q})\langle l_1\vec{k}+\vec{q}\,|\,l_4\vec{k}\rangle\langle l_2\vec{k}'-\vec{q}\,|\,l_3\vec{k}'\rangle \times a^\dagger_{l_1\vec{k}+\vec{q}\sigma}a^\dagger_{l_2\vec{k}'-\vec{q}\sigma'}a_{l_3\vec{k}'\sigma'}a_{l_4\vec{k}\sigma}. \quad (2.5)$$

Here $a^\dagger_{l\vec{k}\sigma}$, $a_{l\vec{k}\sigma}$, and $\xi_l(\vec{k})$ are the creation operator, the annihilation operator, and the electron energy, respectively, for the electron with the band index l, the wave vector $\vec{k}$, and the spin σ: The electron energy is measured from the Fermi level assuming thermal equilibrium initially. $b^\dagger_{\nu\vec{q}}$, $b_{\nu\vec{q}}$, and $\omega_\nu(\vec{q})$ are the creation operator, the annihilation operator, and the phonon energy, respectively, for the phonon with the mode index ν and the wave vector $\vec{q}$. With V as the crystal volume, $g_\nu(\vec{q})/\sqrt{V}$ and $v(\vec{q})/V$ are the electron-phonon coupling constant and the Fourier component of the unscreened Coulomb potential, respectively. $g_\nu(\vec{q})$ is dependent on the band index l though not explicitly shown. $\langle l_i\vec{k}_i\,|\,l_j\vec{k}_j\rangle$ is the overlap integral between the modulating parts of the Bloch functions $|l_i\vec{k}_i\rangle$ and $|l_j\vec{k}_j\rangle$, which are normalized over the crystal volume: We take $\langle l\vec{k}_i\,|\,l\vec{k}_j\rangle=1$ for the intraband matrix. $v(\vec{q})$ is given by

$$v(\vec{q})=\frac{4\pi e^2}{q^2}, \quad (2.6)$$

where e is the electronic charge. As for $g_\nu(\vec{q})$, we consider the piezoelectric scattering (PE), the acoustic deformation potential scattering (AC), the nonpolar optical deformation potential scattering (NPO), and the polar optical-phonon scattering (PO). The former two and the latter two are for the acoustic-phonon modes and for the optical-phonon modes, respectively. In Table I we give the expressions[9] of $|g_\nu(\vec{q})|^2$ for those scatterings, using definitions in Table II. It is to be noted that in Eq. (2.4) we consider the intraband phonon scattering only and neglect the interband one. The electron-phonon interaction leads to the electron-electron interaction via emission and reabsorption of phonons.

Let us consider the temperature Green's function $\mathcal{G}(l\vec{k},i\omega_m)$ with $\omega_m=(2m+1)\pi T$ for the electrons in the band l, where m and T are an integer and the thermal energy, respectively. The function is given[12,13] in the form

$$\mathcal{G}(l\vec{k},i\omega_m)=\frac{1}{i\omega_m-\xi_l(\vec{k})-\Sigma(l\vec{k},i\omega_m)} \quad (2.7)$$

using the self-energy $\Sigma(l\vec{k},i\omega_m)$. This self-energy is given on the basis of the electron-electron interactions both via the Coulomb potential and via the phonon emission and reabsorption, as shown in Fig. 1. Here we use the free-particle Green's functions

$$\mathcal{G}_0(l\vec{k},i\omega_m)=\frac{1}{i\omega_m-\xi_l(\vec{k})} \quad (2.8)$$

and

$$\mathcal{D}_0(\nu\vec{q},i\omega_n)=-\frac{2\omega_\nu(\vec{q})}{\omega_n^2+[\omega_\nu(\vec{q})]^2} \quad (2.9)$$

TABLE II. Definitions.

P_{PE}	Dimensionless isotropic piezoelectric constant $\lvert P_{PE}\rvert^2=\frac{h_{14}^2}{35}\left(\frac{12}{c_l}+\frac{16}{c_t}\right)$
h_{14}	Piezoelectric stress tensor
c	$=\frac{1}{5}(3c_{11}+2c_{12}+4c_{44})$
c_t	$=\frac{1}{5}(c_{11}-c_{12}+3c_{44})$
$\bar{c}$	$=\frac{1}{3}c_l+\frac{2}{3}c_t$
c_{11},c_{12},c_{14}	Elastic stiffness constant
Ξ	Effective deformation potential
E_{NPO}	Optical deformation potential
$(\epsilon^*)^{-1}$	$=\epsilon_\infty^{-1}-\epsilon_0^{-1}$
ϵ_∞	High-frequency dielectric constant

for the electrons and for the phonons, respectively, where $\omega_m=(2m+1)\pi T$ and $\omega_n=2n\pi T$ with integers m and n. In Fig. 1 spins are conserved for each scattering from $l_1\vec{k}+\vec{q}$ to $l_4\vec{k}$ and from $l_2\vec{k}'-\vec{q}$ to $l_3\vec{k}'$. For the Coulomb potential interaction the overlap integrals are assigned to each vertex.

To now take into account the screening effect of the band electrons, we replace the Coulomb potential interaction and the phonon emission and reabsorption interaction vertices in Fig. 1 with the structure illustrated in Fig. 2. We take each free-electron-hole bubble to be made up of the Green's functions for the same band provided that at least one of the vertices connected to the bubble is for the phonon emission and reabsorption interaction. On the other hand, we take various pairs of the Green's functions for the different bands as well as for the same bands if the Coulomb potential interaction vertices only are connected to the bubble. For each bubble we obtain

$$V\chi_{ll'}(\vec{q},i\omega_n)=2T\sum_{\vec{k}m}\mathcal{G}_0(l\vec{k},i\omega_m)\,\mathcal{G}_0(l'\vec{k}+\vec{q},i\omega_m+i\omega_n)\times|\langle l\vec{k}|l'\vec{k}+\vec{q}\rangle|^2. \tag{2.10}$$

Hereafter we replace sum $\sum_{\vec{k}}\cdots$ by an integral $[V/(2\pi)^3]\int d\vec{k}\cdots$. $\chi_{ll'}(\vec{q},i\omega_n)$ is known[12] to be reduced to

$$\chi_{ll'}(\vec{q},i\omega_n)=-2\int\frac{d\vec{k}}{(2\pi)^3}\frac{\Theta(\xi_{l'}(\vec{k}+\vec{q}))-\Theta(\xi_l(\vec{k}))}{i\omega_n-\xi_{l'}(\vec{k}+\vec{q})+\xi_l(\vec{k})}\times|\langle l\vec{k}|l'\vec{k}+\vec{q}\rangle|^2, \tag{2.11}$$

where $\Theta(\omega)$ is the Fermi-Dirac distribution function

$$\Theta(\omega)=\frac{1}{\exp(\omega/T)+1}. \tag{2.12}$$

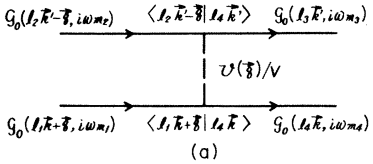

FIG. 1. Illustration of the electron-electron interactions via the Coulomb potential (a) and via the phonon-emission reabsorption (b). $\mathcal{G}_0(l\vec{k},i\omega m)$ and $\mathcal{D}_0(\iota\vec{q},i\omega_n)$ are the free-particle Green's functions for the electrons and the phonons, respectively.

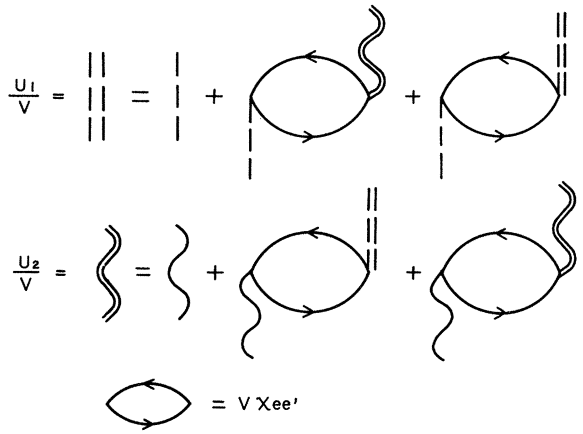

FIG. 2. Modified Coulomb potential interaction U_1/V and the modified phonon emission and reabsorption interaction U_2/V, which describe coupled motion of the band electrons and the phonons.

Let us define

$$\chi(\vec{q},i\omega_n)=\sum_{ll'}\chi_{ll'}(\vec{q},i\omega_n), \tag{2.13}$$

$$\epsilon_0(\vec{q},i\omega_n)=1-v(\vec{q})\sum_{l\neq l'}\chi_{ll'}(\vec{q},i\omega_n), \tag{2.14}$$

$$\epsilon(\vec{q},i\omega_n)=1-v(\vec{q})\chi(\vec{q},i\omega_n). \tag{2.15}$$

Replacing $i\omega_n$ by real ω, $\epsilon_0(\vec{q},\omega)$ and $\epsilon(\vec{q},\omega)$ are the dielectric constant of the host lattice and the free-carrier screening constant plus $\epsilon_0(\vec{q},\omega)$. Noting the definitions of U_1/V and U_2/V in Fig. 2, we obtain the effective electron-electron interaction defined as $U(\vec{q},i\omega_n)/V$, where $U(\vec{q},i\omega_n)=U_1+U_2$. Both U_1 and U_2 are solved using the diagrams in Fig. 2. Considering for the moment a given phonon mode ν, we obtain

$$U(\vec{q},i\omega_n)=\frac{v(\vec{q})}{\epsilon(\vec{q},i\omega_n)}+\left(\frac{\epsilon_0(\vec{q},i\omega_n)}{\epsilon(\vec{q},i\omega_n)}\right)^2|g_\nu(\vec{q})|^2\mathcal{D}(\nu\vec{q},i\omega_n), \tag{2.16}$$

where $\mathcal{D}(\vec{q},i\omega_n)$ is the dressed-phonon Green's function

$$\mathcal{D}(\vec{q},i\omega_n)=\mathcal{D}_0(\vec{q},i\omega_n)\left(1-\frac{\epsilon_0(\vec{q},i\omega_n)}{\epsilon(\vec{q},i\omega_n)}|g_\nu(\vec{q})|^2\times\mathcal{D}_0(\nu\vec{q},i\omega_n)\chi(\vec{q},i\omega_n)\right)^{-1}. \tag{2.17}$$

As seen later, we find that $\mathcal{D}(\vec{q},i\omega_n)=\mathcal{D}_0(\vec{q},i\omega_n)$ is a good approximation. To take into account all the phonon modes is therefore only to sum the second term of Eq. (2.16) over ν. We obtain

$$U(\vec{q}, i\omega_n) = \frac{v(\vec{q})}{\epsilon(\vec{q}, i\omega_n)} + \left(\frac{\epsilon_0(\vec{q}, i\omega_n)}{\epsilon(\vec{q}, i\omega_n)}\right)^2 \sum_{\nu} |g_\nu(\vec{q})|^2 \mathfrak{D}_0(\nu\vec{q}, i\omega_n) . \tag{2.18}$$

The first term and the second term of the equation are the screened Coulomb potential interaction and the screened phonon emission and reabsorption interaction. It is to be noted that if the interband scattering is considered we should take $g_\nu(\vec{q}) = 0$ in Eq. (2.18).

Now we go into the discussion of the minority-carrier lifetime of the Auger recombination. Let us consider an electron in a state $(l_1\vec{k}_1\sigma_1)$, which loses its energy as it interacts with other electrons and phonons. The lifetime of the $(l_1\vec{k}_1\sigma_1)$ state can be calculated on the basis of the self-energy $\Sigma(l_1\vec{k}_1, i\omega_{m_1})$ defined in Eq. (2.7). This self-energy is made up of the structure illustrated in Fig. 3. We write $\Sigma = \Sigma_1 + \Sigma_2 + \cdots$ for the first order, the second order terms, and so on in U: Σ_{1a} refers to the diagram (a) of Σ_1 as an example. The retarded Green's function $G^R(l_1\vec{k}_1, \omega_1)$ is obtained from $\mathcal{G}(l_1\vec{k}_1, i\omega_{m_1})$ replacing $i\omega_{m_1}$ by $\omega_1 + i\delta$ with $\delta \to 0+$ as

$$G^R(l_1\vec{k}_1, \omega_1) = \frac{1}{\omega_1 - \xi_{l_1}(\vec{k}_1) - \Sigma^R(l_1\vec{k}_1, \omega_1)} . \tag{2.19}$$

Here $\Sigma^R(l_1\vec{k}_1, \omega_1)$ is defined by

$$\Sigma^R(l_1\vec{k}_1, \omega_1) = \lim_{\delta \to 0+} \Sigma(l_1\vec{k}_1, \omega_1 + i\delta) . \tag{2.20}$$

Then $\hbar$ times the damping rate of the $(l_1\vec{k}_1\sigma_1)$ state is given by

$$\Gamma(l_1\vec{k}_1, \omega) = -\mathrm{Im}\Sigma^R(l_1\vec{k}_1, \omega_1) . \tag{2.21}$$

Consider hereafter the Auger transition in a direct-gap semi-conductor of p type, where a given electron 1 recombines with a hole 4 exciting an electron 2 to another hole state 3, as shown in Fig. 4: This process is denoted as the 1432 process. Considering the conduction band (CB), the heavy hole band (HB), the light hole band (LB), and the spin split-off band (SB), various transition processes exist such as CHHS, CHHL, CHHH, and so on. Among them the CHHS process (see Fig. 4) may be predominant[8] in a p-type semiconductor so that only this process is considered. It is to be noted that the bands we consider have no definite $\vec{k}$ dependence since $\vec{k}$ is no longer a good quantum number owing to the phonon scattering. In this situation the Green's-function formalism for the Auger process is appropriate. This is done on the basis of Eq. (2.21) starting from the fact that in U the lowest-order term of $\Sigma(l_1\vec{k}_1, i\omega_{m_1})$ for the Auger process is the second-order one, i.e., $\Sigma_2(l_1\vec{k}_1, i\omega_{m_1})$ shown in Fig. 3. Out of the diagrams for $\Sigma_2(l_1\vec{k}_1, i\omega_{m_1})$ two diagrams $\Sigma_{2a}(l_1\vec{k}_1, i\omega_{m_1})$ and $\Sigma_{2b}(l_1\vec{k}, i\omega_{m_1})$ are found to represent the process under consideration. To include higher-order terms we replace the free-particle Green's functions $\mathcal{G}_0$'s in Σ_{2a} and Σ_{2b} by the complete Green's functions $\mathcal{G}$'s as shown in Fig. 5. From this figure we obtain

$$\Sigma_{2a}(l_1\vec{k}_1, i\omega_{m_1}) = -2T^2 \int \frac{d\vec{k}_3}{(2\pi)^3} \int \frac{d\vec{k}_4}{(2\pi)^3} \sum_{m_3 m_4} [U(\vec{k}_4 - \vec{k}_1, i\omega_{m_4} - i\omega_{m_1})]^2 |\langle l_1\vec{k}_1 | l_4\vec{k}_4 \rangle|^2 |\langle l_2\vec{k}_2 | l_3\vec{k}_3 \rangle|^2 \times \mathcal{G}(l_4\vec{k}_4, i\omega_{m_4}) \mathcal{G}(l_3\vec{k}_3, i\omega_{m_3}) \mathcal{G}(l_2\vec{k}_2, i\omega_{m_3} + i\omega_{m_4} - i\omega_{m_1}) , \tag{2.22}$$

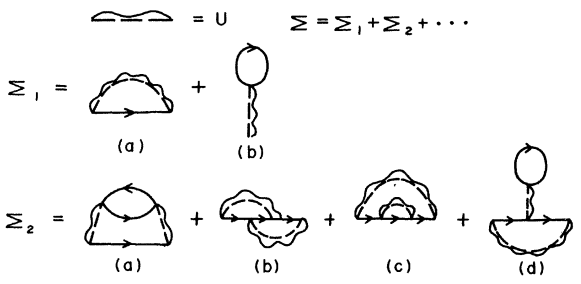

FIG. 3. Diagrams for the self-energy $\Sigma = \Sigma_1 + \Sigma_2 + \cdots$, where Σ_1 and Σ_2 are for the first-order and the second-order terms, respectively, in $U(= U_1 + U_2)$, i.e., the effective electron-electron interaction.

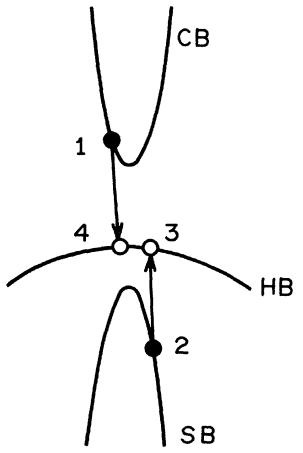

FIG. 4. Auger recombination via the CHHS process among the conduction band, heavy-hole band, and the spin split-off band.

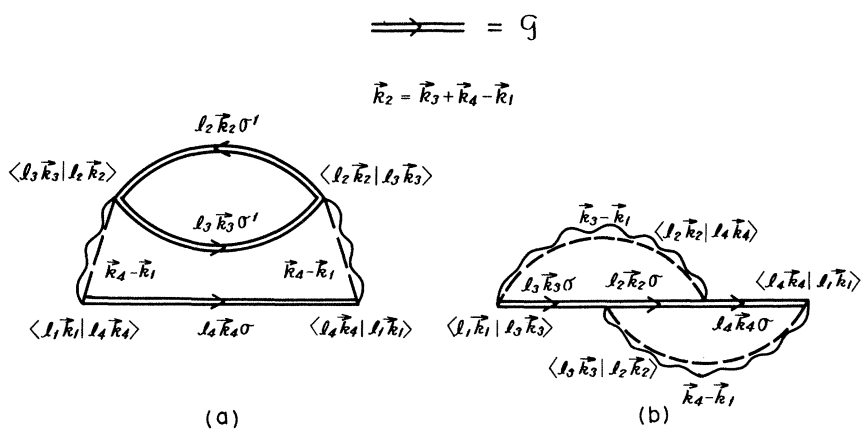

FIG. 5. Diagrams for the self-energy representing the Auger transition recombination.

$$\Sigma_{2b}(l_1\vec{k}_1, i\omega_{m_1}) = T^2 \int \frac{d\vec{k}_3}{(2\pi)^3} \int \frac{d\vec{k}_4}{(2\pi)^3} \sum_{m_3 m_4} U(\vec{k}_3-\vec{k}_1, i\omega_{m_3}-i\omega_{m_1}) U(\vec{k}_4-\vec{k}_1, i\omega_{m_4}-i\omega_{m_1})$$
$$\times \langle l_1\vec{k}_1 | l_3\vec{k}_3\rangle\langle l_3\vec{k}_3 | l_2\vec{k}_2\rangle\langle l_2\vec{k}_2 | l_4\vec{k}_4\rangle\langle l_4\vec{k}_4 | l_1\vec{k}_1\rangle|$$
$$\times \mathcal{G}(l_4\vec{k}_4, i\omega_{m_4}) \mathcal{G}(l_3\vec{k}_3, i\omega_{m_3}) \mathcal{G}(l_2\vec{k}_2, i\omega_{m_3}+i\omega_{m_4}-i\omega_{m_1}) . \quad (2.23)$$

Hereafter we use the notation $\vec{k}_2 = \vec{k}_3 + \vec{k}_4 - \vec{k}_1$. The factor 2 in front of the summation in Eq. (2.22) comes from summing over σ' in Fig. 5(a). Since we are considering the interband transition as shown in Fig. 4, each U in Eqs. (2.22) and (2.23) is only the first term of Eq. (2.16), i.e., v/ϵ. On the other hand, if we consider some other processes including the intraband transition, e.g., the CHHH process, the second term should also be included though this is much smaller than the first term.

It is assumed here that we can make approximations $\epsilon_0(\vec{q}, \omega) = \epsilon_0(0, 0)$ and $\epsilon(\vec{q}, \omega) = \epsilon(\vec{q}, 0)$, which are denoted simply as ϵ_0 and $\epsilon(\vec{q})$, respectively. The approximation for ϵ_0 will be good as long as we consider the transitions involving only small wave-vector changes and small energy changes, i.e., $|\vec{k}_4 - \vec{k}_1| \ll \pi/a$ (a is the lattice constant), $|\vec{k}_3 - \vec{k}_2| \ll \pi/a$, $|E_4 - E_1| \simeq E_G$, and $|E_3 - E_2| \simeq E_G$. This condition is satisfied for the present case of the Auger transition in a direct-gap material. For an indirect-gap material, however, wave-vector changes of the order of π/a are involved as important processes: For these processes we should take $\epsilon_0 = 1$. On the other hand, the approximation for $\epsilon(\vec{q}, \omega)$ will be good as far as the energy changes are well below the thermal energy. Although this condition is not satisfied, we use $\epsilon(\vec{q})$ in view of that the free-carrier screening is not so important an effect for the Auger process.

It is convenient to replace the sums over m and n in Eqs. (2.22) and (2.23) with contour integrations. We perform this integration noting the assumption of the ω independent $\epsilon(\vec{q})$. Then we make use of the analytical relations among the temperature, the retarded, and the advanced Green's functions. Noting Eq. (2.21) and taking into account all possible ways of assigning $(l_2\vec{k}_2)$, $(l_3\vec{k}_3)$, and $(l_4\vec{k}_4)$ to three Green's functions in the diagrams of Fig. 5, we obtain

$$\Gamma(l_1\vec{k}_1, \omega_1) = \frac{2}{\pi^2} \int \frac{d\vec{k}_3}{(2\pi)^3} \int \frac{d\vec{k}_4}{(2\pi)^3} (|f|^2 + |g|^2 + |f-g|^2)$$
$$\times \int d\omega_3 \int d\omega_4 \{\Theta(\omega_2)[1-\Theta(\omega_3)][1-\Theta(\omega_4)] + [1-\Theta(\omega_2)]\Theta(\omega_3)\Theta(\omega_4)\}$$
$$\times \mathrm{Im}G^R(l_2\vec{k}_2, \omega_2)\, \mathrm{Im}G^R(l_3\vec{k}_3, \omega_3)\, \mathrm{Im}G^R(l_4\vec{k}_4, \omega_4) . \quad (2.24)$$

Here $\vec{k}_2 = \vec{k}_3 + \vec{k}_4 - \vec{k}_1$, $\omega_2 = \omega_3 + \omega_4 - \omega_1$,

$$f = \langle l_1\vec{k}_1 | l_4\vec{k}_4\rangle\langle l_2\vec{k}_2 | l_3\vec{k}_3\rangle v(\vec{k}_4-\vec{k}_1)/\epsilon(\vec{k}_4-\vec{k}_1) , \quad (2.25)$$

$$g = \langle l_1\vec{k}_1 | l_3\vec{k}_3\rangle\langle l_2\vec{k}_2 | l_4\vec{k}_4\rangle v(\vec{k}_3-\vec{k}_1)/\epsilon(\vec{k}_3-\vec{k}_1) , \quad (2.26)$$

and $\Theta(\omega)$ is the Fermi-Dirac distribution function defined by Eq. (2.12).

It is to be noted that the damping $\Gamma(l_1\vec{k}_1, \omega_1)$ of the electron in the $(l_1\vec{k}_1\sigma_1)$ state has been determined for a system in thermal equilibrium. In

order to calculate the minority-carrier lifetime we consider departure from the equilibrium. It is assumed that this departure is infinitesimally small and that in nonequilibrium state quasiequilibrium exists among the electrons of the CB and among those of the valence band (VB), but not between the CB and the VB. This is taken into account by using quasi-Fermi levels for the CB and the VB. Equation (2.24) is used as an approximation for $\Gamma(l_1\vec{k}_1, \omega_1)$, considering that the energies $\xi_{l_i}(\vec{k}_i)$'s $(i=1,2,3,4)$ involved in the equation are measured from the quasi-Fermi level for the VB: The approximation is valid up to the zeroth order in the departure from the equilibrium. The density of states $\rho(l_1\vec{k}_1, \omega_1)$ for the CB electrons, which are the minority carriers, are given[14] in the same approximation by

$$\rho(l_1\vec{k}_1, \omega_1) = -2\,\mathrm{Im}G^R(l_1\vec{k}_1, \omega_1)\,. \tag{2.27}$$

The distribution for those carriers is described by $\Theta(\omega_1 - F_1)$, where F_1 is the quasi-Fermi level for the CB measured from that for the VB and $\Theta(\omega)$ has been defined by Eq. (2.12). The average lifetime τ of the minority carriers is

$$\frac{1}{\tau} = \frac{1}{\hbar}\int \frac{d\vec{k}_1}{(2\pi)^3}\int d\omega_1 \Gamma(l_1\vec{k}_1, \omega_1)\rho(l_1\vec{k}_1, \omega_1)\Theta(\omega_1 - F_1) \Big/ \int \frac{d\vec{k}_1}{(2\pi)^3}\int d\omega_1 \rho(l_1\vec{k}_1, \omega_1)\Theta(\omega_1 - F_1)\,. \tag{2.28}$$

The minority-carrier concentration n is defined by

$$n = \int \frac{d\vec{k}_1}{(2\pi)^3}\int d\omega_1 \rho(l_1\vec{k}_1, \omega_1)\Theta(\omega_1 - F_1)\,. \tag{2.29}$$

Using this relation and Eq. (2.27) we obtain

$$\begin{aligned}\frac{1}{\tau} = \frac{1}{n}\frac{4}{\hbar}\frac{1}{\pi^2}\int \frac{d\vec{k}_1}{(2\pi)^3}\int \frac{d\vec{k}_3}{(2\pi)^3}\int \frac{d\vec{k}_4}{(2\pi)^3}(|f|^2 + |g|^2 + |f-g|^2) \\ \times \int d\omega_1 \int d\omega_2 \int d\omega_3 F(\omega_1, \omega_2, \omega_3, \omega_4) \\ \times \mathrm{Im}G^R(l_1\vec{k}_1, \omega_1)\,\mathrm{Im}G^R(l_2\vec{k}_2, \omega_2)\,\mathrm{Im}G^R(l_3\vec{k}_3, \omega_3)\,\mathrm{Im}G^R(l_4\vec{k}_4, \omega_4)\,,\end{aligned} \tag{2.30}$$

where

$$F(\omega_1, \omega_2, \omega_3, \omega_4) = \{\Theta(\omega_2)[1-\Theta(\omega_3)][1-\Theta(\omega_4)] + [1-\Theta(\omega_2)]\Theta(\omega_3)\Theta(\omega_4)\}\Theta(\omega_1 - F_1)\,. \tag{2.31}$$

Using Eq. (2.19) τ is calculated from Eq. (2.30) once $\Sigma^R(l\vec{k}, \omega)$ is determined as in the next section.

III. APPROXIMATE FORMULA FOR NUMERICAL CALCULATION

In this section Eq. (2.30) is cast into more tractable form. First we note that $\mathrm{Im}G^R(l\vec{k}, \omega)$ represents a discrete state at $\omega = \xi_l(\vec{k})$ broadened with the width of $|\mathrm{Im}\Sigma^R(l\vec{k}, \omega)|$. As seen later, this width is much smaller than the electron energy of interest, showing free-particle-like behavior of the electrons. Further, since as seen later the width is proportional to the effective mass of the band under consideration, the electrons in the CB and the SB are much more free-particle-like than those in the HB. Thus we approximate G^R by G_0^R for the CB and the SB. Let us write $G^R(i) = G_0^R(i) + G_r^R(i)$, where we use the abbreviation $i \equiv l_i\vec{k}_i, \omega_i$ and $G_r^R(i)$ is the sum of the higher-order terms in $\Sigma^R(i)$ other than the zeroth. We obtain

$$\begin{aligned}\mathrm{Im}G^R(1)\mathrm{Im}G^R(2)\mathrm{Im}G^R(3)\mathrm{Im}G^R(4) = \mathrm{Im}G_0^R(1)\mathrm{Im}G_0^R(2)\,[\mathrm{Im}G^R(3)\mathrm{Im}G_0^R(4) + \mathrm{Im}G_0^R(3)\mathrm{Im}G^R(4) \\ - \mathrm{Im}G_0^R(3)\mathrm{Im}G_0^R(4) + \mathrm{Im}G_r^R(3)\mathrm{Im}G_r^R(4)]\,.\end{aligned} \tag{3.1}$$

From the above discussions we neglect the last term in the square brackets. The neglect of this term will lead to underestimation of $1/\tau$. Noting $\mathrm{Im}G_0^R(l_i\vec{k}_i, \omega_i) = -\pi\delta(\omega_i - \xi_i)$, where we use the abbreviation $\xi_i = \xi_{l_i}(\vec{k}_i)$, and the symmetric property of the integrand in Eq. (2.30) with respect to an interchange of $\vec{k}_3$ $(\vec{k}_4)$ to $\vec{k}_4$ $(\vec{k}_3)$, Eq. (2.30) becomes

$$\begin{aligned}\frac{1}{\tau} = -\frac{4\pi}{\hbar}\frac{1}{n}\int \frac{d\vec{k}_1}{(2\pi)^3}\int \frac{d\vec{k}_3}{(2\pi)^3}\int \frac{d\vec{k}_4}{(2\pi)^3}(|f|^2 + |g|^2 + |f-g|^2)F(\xi_1, \xi_2, \xi_1 + \xi_2 - \xi_4, \xi_3) \\ \times [2\,\mathrm{Im}G^R(l_3\vec{k}_3, \xi_1 + \xi_2 - \xi_4) + \pi\delta(\xi_1 + \xi_2 - \xi_3 - \xi_4)]\,.\end{aligned} \tag{3.2}$$

Especially when $\mathrm{Im}G^R(l_3\vec{k}_3, \xi_1+\xi_2-\xi_4) = \mathrm{Im}G_0^R(l_3\vec{k}_3, \xi_1+\xi_2-\xi_4) \equiv -\pi\delta(\xi_1+\xi_2-\xi_3-\xi_4)$, we obtain the well known expression for the lifetime of the pure collision Auger recombination.

We are now at the position to calculate $\Sigma^R(l\vec{k}, \omega)$. The real part of $\Sigma^R(l\vec{k}, \omega)$ represents the energy shift and is considered to give mainly changes of E_G and Δ_0. In view of the fact that we use the experimental data of E_G and Δ_0 in practical calculation, we neglect hereafter the real part of $\Sigma^R(l\vec{k}, \omega)$. On the other hand, the imaginary part of $\Sigma^R(l\vec{k}, \omega)$ gives the broadening of the discrete free-particle state and its contribution to the lifetime is the present theme. The lowest-order diagrams for $\Sigma^R(l\vec{k}, \omega)$ are $\Sigma_{1a}^R(l\vec{k}, \omega)$ and $\Sigma_{1b}^R(l\vec{k}, \omega)$, which are obtained from $\Sigma_{1a}(l\vec{k}, i\omega_m)$ and $\Sigma_{1b}(l\vec{k}, i\omega_m)$, respectively, shown in Fig. 3 by replacing $i\omega_m$ with $\omega+i\delta$. Only $\Sigma_{1a}^R(l\vec{k}, \omega)$ has an imaginary part and is considered. First we have

$$\Sigma_{1a}(l\vec{k}, i\omega_m) = -T\int\frac{d\vec{q}}{(2\pi)^3}\sum_n U(\vec{k}-\vec{q}, i\omega_m - i\omega_n)\mathcal{G}_0(l\vec{k}, i\omega_n)\,. \tag{3.3}$$

Replacing the sum over n by the contour integration and using Eq. (2.18) and the analytical relations for the Green's functions as $D_0^R(l\vec{k}, \omega) = \mathfrak{D}_0(l\vec{k}, \omega+i\delta)$ and $G_0^R(l\vec{k}, \omega) = \mathcal{G}_0(l\vec{k}, \omega+i\delta)$, we obtain

$$\mathrm{Im}\Sigma_{1a}^R(l\vec{k}, \omega) = -\sum_\nu\int\frac{d\vec{q}}{(2\pi)^3}\left(\frac{\epsilon_0}{\epsilon(\vec{k}-\vec{q})}\right)^2 |g_\nu(\vec{k}-\vec{q})|^2\{\delta(\omega-\omega_\nu(\vec{k}-\vec{q})-\xi_l(\vec{q}))[P(\omega_\nu(\vec{k}-\vec{q}))+2] + \delta(\omega+\omega_\nu(\vec{k}-\vec{q})-\xi_l(\vec{q}))[P(\omega_\nu(\vec{k}-\vec{q}))-1]\}, \tag{3.4}$$

where

$$P(\omega) = \frac{1}{\exp(\omega/\tau)-1} \tag{3.5}$$

is the number of phonons with energy ω. In order to see the degree of relative importance of $\mathrm{Im}\Sigma_2^R(l\vec{k}, \omega)$ with respect to $\mathrm{Im}\Sigma_{1a}^R(l\vec{k}, \omega)$, we estimate the intraband-scattering part of $\mathrm{Im}\Sigma_2^R(l\vec{k}, \omega)$ taking $\mathrm{Im}\Sigma_{2a}^R(l\vec{k}, \omega)$ as an example. This is given by

$$\mathrm{Im}\Sigma_{2a}^R(l\vec{k}, \omega) = 2\pi\int\frac{d\vec{k}_3}{(2\pi)^3}\int\frac{d\vec{k}_4}{(2\pi)^3}\delta(\xi+\zeta_2-\zeta_3-\zeta_4) \times\{\Theta(\zeta_2)[1-\Theta(\zeta_3)][1-\Theta(\zeta_4)]+[1-\Theta(\zeta_2)]\Theta(\zeta_3)\Theta(\zeta_4)\}[U^A(\vec{k}_4-\vec{k}_1, \zeta_2-\zeta_3)]^2\,. \tag{3.6}$$

where $\zeta = \xi_l(\vec{k})$, $\zeta_i = \xi_l(\vec{k}_i)$ $(i=2,3,4)$, $\vec{k}_2 = \vec{k}_3+\vec{k}_4-\vec{k}_1$, and $U^A(\vec{q}, \omega)$ is obtained from Eq. (2.18) by replacing $\mathfrak{D}_0(\vec{q}, i\omega_n)$ with the advanced Green's function $D_0^A(\nu\vec{q}, \omega)$: $\epsilon(\vec{q}, i\omega_n)$ and $\epsilon_0(\vec{q}, i\omega_n)$ are also replaced with $\epsilon(\vec{q})$ and ϵ_0 as has been indicated. We will show later by comparing $\mathrm{Im}\Sigma_{2a}^R(l\vec{k}, \omega)$ with $\mathrm{Im}\Sigma_{1a}^R(l\vec{k}, \omega)$ that to take $\mathrm{Im}\Sigma^R(l\vec{k}, \omega) = \mathrm{Im}\Sigma_{1a}^R(l\vec{k}, \omega)$ is a good approximation.

Here we assume spherical energy surfaces for the CB, HB, and SB and define the effective masses m_C, m_H, and m_S, respectively, for those bands: The energies measured from the respective band edges upward (CB) or downward (HB and SB) are given by $\hbar^2k^2/2m_l$ with $l=C$, H, and S; m_l is dependent on $\vec{k}$. For a p-type semiconductor under consideration we calculate $\chi_{ll}(0,0)$ from Eq. (2.11). This corresponds to the Thomas-Fermi approach which is valid at high carrier concentrations. Then we obtain

$$\epsilon(\vec{q}) = \epsilon_0\left(1+\frac{\lambda^2}{q^2}\right), \tag{3.7}$$

where λ is the inverse screening length given as

$$\lambda^2 = \frac{2\pi pe^2}{\epsilon_0 T}\frac{F_{-1/2}(\eta_p)}{F_{1/2}(\eta_p)}\,. \tag{3.8}$$

Here p is the hole concentration, $T\eta_p$ the quasi-Fermi level for the VB measured downward from the VB edge, and

$$F_a(b) = \int_0^\infty dx\frac{x^a}{\exp(x-b)+1} \tag{3.9}$$

the Fermi integral.

On this basis we first examine various approximations which have been made. Hereafter we consider p-GaAs and p-GaSb as typical materials in that they have $E_G \gg \Delta_0$ and $E_G \simeq \Delta_0$, respectively. Material parameters are listed in Table III. We first discuss Eq. (2.17) using the inequality $-\mathfrak{D}_0(\nu\vec{q}, i\omega_n) \le 2/\omega_\nu(\vec{q})$ [see Eqs. (2.9), (2.6), and (2.15)]. We obtain for the second term in the large parentheses of Eq. (2.17)

$$-[\epsilon_0/\epsilon(\vec{q})]|g_\nu(\vec{q})|^2\mathfrak{D}_0(\nu\vec{q}, i\omega_n)\chi(\vec{q}, 0) \quad (\equiv t_2 > 0)$$

as

$$t_2 < \frac{\epsilon_0 q^2}{4\pi e^2}\frac{\epsilon(\vec{q})-1}{\epsilon(\vec{q})}\frac{2}{\omega_\nu(\vec{q})}|g_\nu(\vec{q})|^2\,. \tag{3.10}$$

TABLE III. Material parameters.

Parameter		GaAs	GaSb
E_G (eV)	77 K	1.511	0.784
E_G (eV)	150 K	1.455	0.758
E_G (eV)	300 K	1.428	0.700
Δ_0 (eV)	77 K	0.34	0.757
Δ_0 (eV)	150 K	0.34	0.771
Δ_0 (eV)	300 K	0.34	0.800
m_C/m_0		0.0673	0.0472
m_H/m_0		0.536	0.371
m_S/m_0 ($\vec{k}=0$)		0.138	0.130
ϵ_0		13.18	15.69
$(\epsilon^*)^{-1}$		0.0159	0.005 52
c_l (10^{12} dyn/cm^2)		1.397	1.037
c_t (10^{12} dyn/cm^2)		0.486	0.355
$\bar{c}$ (10^{12} dyn/cm^2)		0.790	0.582
h_{14} (10^4 esu)		4.83	3.17
P_{PE}		0.0526	0.0403
Ξ (eV)		6.6	6.9
E_{NPO} (eV)		6.5	5.9
ω_{OP} (eV)		0.0296	0.0298

Noting $\epsilon(\vec{q}) \gg 1$ and using the material parameters given in Table III, we find $t_2 < 0.1$ in the range $q < 10^7$ cm^{-1}. Therefore t_2 is negligible in Eq. (2.17), as has been stated. As for Eq. (2.18) we consider the ratio r of the second term to the first. We obtain

$$|r| < \frac{\epsilon_0 q^2}{4\pi e^2} \sum_\nu \frac{2}{\omega_\nu(\vec{q})} |g_\nu(\vec{q})|^2 \tag{3.11}$$

and find $|r| < 0.3$ in the range $q < 10^7$ cm^{-1}. Therefore the second term of Eq. (2.18) is almost negligible even for the intraband scattering as compared to the first one.

Let us calculate Eq. (3.4) neglecting the phonon energy $\omega_\nu(\vec{k}-\vec{q})$ as compared to the electron energy $\xi_l(\vec{q})$ in the δ functions. In the calculation we treat four phonon scatterings separately. We assume the optical phonon energy ω_{OP} to be independent of the wave vector and make a reasonable approximation $[1+2p(\omega_{\mathrm{AC}})] = 2T/\omega_{\mathrm{AC}}$ for the acoustic-phonon energy ω_{AC}. Using Eq. (3.6) we obtain for the HB

$$\mathrm{Im}\Sigma^R_{1a}(l\vec{k},\omega) = -\frac{2m_H}{\hbar^2}\frac{1}{k}[AH_1(k,k_0)+BH_2(k,k_0)], \tag{3.12}$$

where

$$k_0 = \left(\frac{2m_H}{\hbar^2}(F_p-\omega)\right)^{1/2}, \tag{3.13}$$

$$A = \frac{1}{8\pi}\left(\frac{1}{c_l}\Xi^2 T + \frac{1}{2\bar{c}}E^2_{\mathrm{NPO}}[1+2P(\omega_{\mathrm{OP}})]\right), \tag{3.14}$$

$$B = \frac{1}{8\pi}\left(e^2 P^2_{\mathrm{PE}} T + \frac{2\pi e^2}{\epsilon^*}[1+2P(\omega_{\mathrm{OP}})]\right), \tag{3.15}$$

$$H_1(k,k_0) = 2k_0 k - \lambda^2\left[\ln\left|\frac{(k+k_0)^2+\lambda^2}{(k-k_0)^2+\lambda^2}\right| - \tfrac{1}{2}\lambda^2\left(\frac{1}{(k-k_0)^2+\lambda^2} - \frac{1}{(k+k_0)^2+\lambda^2}\right)\right], \tag{3.16}$$

$$H_2(k,k_0) = \frac{1}{2}\left[\ln\left|\frac{(k+k_0)^2+\lambda^2}{(k-k_0)^2+\lambda^2}\right| - \lambda^2\left(\frac{1}{(k-k_0)^2+\lambda^2} - \frac{1}{(k+k_0)^2+\lambda^2}\right)\right]. \tag{3.17}$$

For Eq. (3.13) the restrictive condition is $F_p - \omega \geq 0$ and F_p is the quasi-Fermi level for the VB measured downward from the VB edge, i.e., $F_p = T\eta_p$. Especially when $k \gg k_0 + \lambda$, we obtain approximately $H_1(k_1,k_0) = 2kk_0$ and $H_2(k,k_0) = 0$. Thus the screening of the electron-phonon interaction can be neglected and the NPO scattering and the AC scattering are especially important.

Equation (3.6) is now calculated for the intraband scattering among heavy holes in order to discuss the effect of the higher-order terms of $\mathrm{Im}\Sigma^R(l\vec{k},\omega)$. As discussed just below Eq. (3.11), we can approximately take $U^A(\vec{k}_4-\vec{k}_1) = v(\vec{k}_4-\vec{k}_1)/\epsilon(\vec{k}_4-\vec{k}_1)$. Considering nondegenerate statics and taking $\omega = \xi[\equiv\xi_l(\vec{k})]$, we obtain

$$\mathrm{Im}\Sigma^R_{2a}(l\vec{k},\zeta) = \frac{\hbar e^4 p}{(2\pi m_H T)^{1/2}\epsilon_0^2\lambda^2} \times \int d\vec{k}_2 \frac{|\vec{k}_2-\vec{k}|^2}{|k_2-k|^2+\lambda^2}\exp\left(-\frac{\hbar^2}{2m_H T}k_2^2\right). \tag{3.18}$$

This is evaluated for two extreme cases $\hbar^2 k_1^2/(2m_H T) \ll 1$ or $\gg 1$ and for the intermediate cases by interpolation. On the other hand, $\mathrm{Im}\Sigma^R_{1a}(l\vec{k},\omega)$ is evaluated from Eqs. (3.12)–(3.17) taking $\omega = \zeta$ $[\equiv\xi_l(\vec{k})]$ also. It is found that the ratio

$$|\mathrm{Im}\Sigma^R_{2a}(l\vec{k},\zeta)/\mathrm{Im}\Sigma^R_{1a}(l\vec{k},\zeta)|$$

decreases with increasing value of k/λ and is below about 0.1 in the range $k/\lambda \gtrsim 0.5$, which is of practical interest. In view of this result the higher-order terms of $\mathrm{Im}\Sigma^R(l\vec{k},\omega)$ other than the first are negligible. Therefore we take

$$\mathrm{Im}\Sigma^R(l\vec{k},\omega) = \mathrm{Im}\Sigma^R_{1a}(l\vec{k},\omega) \tag{3.19}$$

in a good approximation.

Using Eqs. (2.21), (3.19), (3.12)–(3.17), and (3.2), we calculate the minority-carrier lifetime in a p-type semiconductor. For the CHHS process under consideration we have $1-\Theta(\xi_2) \ll 1$ so that we approximately obtain

$$F(\xi_1,\xi_2,\xi_1+\xi_2-\xi_4,\xi_4)$$
$$=[1-\Theta(\xi_1+\xi_2-\xi_4)][1-\Theta(\xi_4)]\Theta(\xi_1-F_1)\,. \quad (3.20)$$

We note here the relations $\xi_1=\hbar^2k_1^2/2m_C+E_G+F_p$, $\xi_2=-\hbar^2k_2^2/2m_S-\Delta_0+F_p$, $\xi_3=-\hbar^2k_3^2/2m_H+F_p$, and $\xi_4=-\hbar^2k_4^2/2m_H+F_p$. Since the Auger transition occurs around the respective band edges for the CB and the HB, m_C and m_H are evaluated at $\vec{k}=0$. On the other hand, m_S is evaluated for the threshold value of k. As for the overlap integral we use the relation[15]

$$|\langle l_i\vec{k}_i|l_j\vec{k}_j\rangle|^2=\frac{\hbar^2}{2m_0}\frac{|\vec{k}_i-\vec{k}_j|}{|\xi_{l_i}(\vec{k}_i)-\xi_{l_j}(\vec{k}_j)|}f_{ij} \quad (3.21)$$

for the interband matrix, where m_0 and f_{ij} are the electron mass in the free space and the oscillator strength, respectively. We make an approximation $|\xi_{l_i}(\vec{k}_i)-\xi_{l_j}(\vec{k}_j)|=E_G$ for the combinations $(i,j)=(1,3)$, $(1,4)$, $(2,3)$, and $(2,4)$. Another approximation is to take $|\vec{k}_i-\vec{k}_j|^2/(|\vec{k}_i-\vec{k}_j|^2+\lambda^2)=1$ in Eqs. (2.25) and (2.26) for f and g and we obtain $|f|^2=|g|^2$. Taking $G^R(l_1\vec{k}_1,\omega_1)=G_0^R(l_1\vec{k},\omega_1)$ in Eq. (2.29) again as an approximation and assuming nondegenerate statistics, we have $n=N_C\exp(F_n/T)$, where $N_C=2(m_CT/2\pi\hbar^2)^{3/2}$ and F_n are the effective density of states and the quasi-Fermi level measured upward from the CB edge, respectively, for the CB. We take approximately[16] $|f|^2+|g|^2+|f-g|^2=2|f|^2$ and change the integration variables $(\vec{k}_1,\vec{k}_3,\vec{k}_4)$ in Eq. (3.2) to $(\vec{k}_1,\vec{k}_2,\vec{k}_4)$ noting the relation $\vec{k}_1+\vec{k}_2-\vec{k}_3-\vec{k}_4=0$. We obtain

$$\frac{1}{\tau}+\frac{1}{\tau_0}=\frac{16\pi}{\hbar}\left(\frac{2\pi e^2\hbar^2}{m_0\epsilon_0E_G}\right)^2\frac{1}{N_C}\exp[(2F_P+E_G-\Delta_0)/T]$$
$$\times\int\frac{d\vec{k}_2}{(2\pi)^3}\int\frac{d\vec{k}_1}{(2\pi)^3}\int\frac{d\vec{k}_4}{(2\pi)^3}f_{CH}f_{SH}\exp(-E_2/T)\Phi(\vec{k}_1,\vec{k}_2,\vec{k}_4)$$
$$\times\frac{1}{1+\exp[(E_1+E_4-E_2+E_G-\Delta_0+F_p)/T]}\frac{1}{1+\exp[(F_p-E_4)/T]} \quad (3.22)$$

under the condition

$$E_2-E_1-E_4-E_G+\Delta_0\geq 0\,, \quad (3.23)$$

where $E_1=\hbar^2k_1^2/2m_C$, $E_2=\hbar^2k_2^2/2m_S$, $E_3=\hbar^2k_3^2/2m_H$, $E_4=\hbar^2k_4^2/2m_H$, $\vec{k}_3=\vec{k}_1+\vec{k}_2-\vec{k}_4$,

$$\Phi(\vec{k}_1,\vec{k}_2,\vec{k}_4)=\frac{-\mathrm{Im}\Sigma_{1a}^R(l_3\vec{k}_3,E_1+E_4-E_2-E_G+\Delta_0+F_p)}{(E_1+E_3+E_4-E_2+E_G-\Delta_0)^2+[\mathrm{Im}\Sigma_{1a}^R(l_3\vec{k}_3,E_1+E_4-E_2-E_G+\Delta_0+F_p)]^2}\,, \quad (3.24)$$

and τ_0 is the minority carrier lifetime of the pure collision Auger process. It is to be pointed out that the right-hand side of Eq. (3.22) is $2/\tau_0$ especially when $-\mathrm{Im}\Sigma_{1a}^R\to 0+$ leading to $\Phi(\vec{k}_1,\vec{k}_2,\vec{k}_4)=\pi\delta(E_1+E_3+E_4-E_2+E_G-\Delta_0)$. Then we obtain $\tau=\tau_0$. Thus the expression for τ involves the pure collision Auger process as a special case.

For facility of numerical calculation, we define $w=(E_2-E_1-E_4-E_G+\Delta_0)/T$, $u=\mu_H(E_2-E_1-E_3-E_4-E_G+\Delta_0)/T$ with $\mu_H=m_C/m_H$, $v=-(\mu_H/T)\,\mathrm{Im}\Sigma_{1a}^R(l_3\vec{k}_3,E_1+E_4-E_2-E_G+\Delta_0+F_P)$, $r\phi=(E_1/T)^{1/2}$, $r(1-\phi^2)^{1/2}=(E_4/T)^{1/2}$, and $r_0=[(E_2-E_G+\Delta_0)/T]^{1/2}$ where $E_2\geq 0$ if $E_G\leq\Delta_0$ and $E_2\geq E_G-\Delta_0$ if $E_G\geq\Delta_0$. Inequality (3.23) corresponds to $r\leq r_0$. Defining ξ and η by $\vec{k}_1\cdot(\vec{k}_2-\vec{k}_4)=\xi k_1|\vec{k}_2-\vec{k}_4|$ and $\vec{k}_2\cdot\vec{k}_4=\eta k_2k_4$, respectively, we obtain

$$\frac{1}{\tau}=\frac{32e^4m_Cm_S^{3/2}m_H^{1/2}T^2}{\pi^{3/2}\hbar^3m_0^2\epsilon_0^2E_G^2}f_{CH}\exp(2\eta_p+z_0-z_1)\int_0^\infty dz(z+z_1)^{1/2}\exp(-z)S(z)f_{SH}-\frac{1}{\tau_0}\,, \quad (3.25)$$

where $z_0=(E_G-\Delta_0)/T$, $z_1=(z_0+|z_0|)/2$, $\eta_p=F_p/T$,

$$S(z)=\int_0^{r_0}dr\,r^2\int_0^1d\phi\,\phi^2(1-\phi^2)^{1/2}\int_{-1}^1d\xi\int_{-1}^1d\eta\frac{v}{u^2+v^2}\frac{1}{1+\exp(\eta_p-w)}\frac{1}{1+\exp[\eta_p-r^2(1-\phi^2)]}\,. \quad (3.26)$$

Here we have

$$r_0=(z+z_1-z_0)^{1/2}\,, \quad (3.27)$$
$$w=r_0^2-r^2\,, \quad (3.28)$$
$$u=\mu_H(w-t)\,, \quad (3.29)$$
$$t=\mu_Hr^2\phi^2+2\xi r\phi(\mu_Hs)^{1/2}+s\,, \quad (3.30)$$
$$s=\frac{m_S}{m_H}(r_0^2+z_0)+r^2(1-\phi^2)-2\eta r\left(\frac{m_S}{m_H}(1-\phi^2)(r_0^2+z_0)\right)^{1/2}\,, \quad (3.31)$$

$$v = A_0 F_A + B_0 F_B \,, \tag{3.32}$$

$$A_0 = \frac{m_C}{4\pi\hbar^2}\left(\frac{2m_H T}{\hbar^2}\right)^{1/2}\left(\frac{1}{c_l}\Xi^2 + \frac{1}{2\bar{c}}E_{\mathrm{NPO}}^2[1+2P(\omega_{\mathrm{OP}})]\frac{\omega_{\mathrm{OP}}}{T}\right), \tag{3.33}$$

$$B_0 = \frac{m_C}{4\pi\hbar^2}\left(\frac{\hbar^2}{2m_H T}\right)^{1/2}\left(e^2 P_{\mathrm{PE}}^2 + \frac{4\pi e^2}{\epsilon^*}[1+2P(\omega_{\mathrm{OP}})]\frac{\omega_{\mathrm{OP}}}{T}\right), \tag{3.34}$$

$$F_A = 2\sqrt{w} - \frac{y_\lambda}{\sqrt{t}}\left[\ln\left|\frac{(\sqrt{w}+\sqrt{t})^2+y_\lambda}{(\sqrt{w}-\sqrt{t})^2+y_\lambda}\right| - \tfrac{1}{2}y_\lambda\left(\frac{1}{(\sqrt{w}-\sqrt{t})^2+y_\lambda} - \frac{1}{(\sqrt{w}+\sqrt{t})^2+y_\lambda}\right)\right], \tag{3.35}$$

$$F_B = \frac{1}{2\sqrt{t}}\left[\ln\left|\frac{(\sqrt{w}+\sqrt{t})^2+y_\lambda}{(\sqrt{w}-\sqrt{t})^2+y_\lambda}\right| - y_\lambda\left(\frac{1}{(\sqrt{w}-\sqrt{t})^2+y_\lambda} - \frac{1}{(\sqrt{w}+\sqrt{t})^2+y_\lambda}\right)\right], \tag{3.36}$$

and $y_\lambda = \hbar^2\lambda^2/2m_H T$. The expression for τ_0 can be written by slight modification of the result in a literature[11] as

$$\frac{1}{\tau_0} = \frac{8\sqrt{2}\,e^4 m_H^{3/2} m_S^{7/2} T^2 a^2 b^{3/2}}{\pi^{3/2}\hbar^3 m_0^2 m_C^2 \epsilon_0^2 E_G^2} f_{\mathrm{CH}} \exp(2\eta_p + z_0 - z_2)$$
$$\times \int_0^\infty dz\,(z+z_2)^{1/2}(z+z_2-z_T)^{3/2} f_{\mathrm{SH}} \exp(-z)$$
$$\times \int_0^1 dx\, x^2\left([(z+z_2-z_T)(1-x^2)]^{1/2} + \frac{m_H}{m_S[ab^3(z+z_2)]^{1/2}}(J_1 - J_2 + \ln J_1 - \ln J_2)\right), \tag{3.37}$$

where $a = m_C/m_S - \mu_H b/2$, $b = (1+\mu_H/2)^{-1}$; $z_T = E_T/T$ with E_T determined from

$$E_T = \left(1 + \frac{\mu_H b}{2a(E_T)}\right)(E_G - \Delta_0)\,, \tag{3.38}$$

$z_2 = (z_T + |z_T|)/2$, and

$$J_{\substack{1\\(2)}} = \left[1 + \exp\left(\eta_p - \frac{m_S}{4m_H}\left\{\left[\left(\frac{a}{b}(z+z_2-z_T)\right)^{1/2} (\mp) b(z+z_2)^{1/2}\right]^2 + \frac{2a}{\mu_H}(z+z_2-z_T)x^2\right\}\right)\right]^{-1}. \tag{3.39}$$

In deriving Eqs. (3.25) and (3.37) we have neglected $(y/m_S)(dm_S/dy)$ ($\ll 1$). In both of those equations f_{SH} is evaluated at $E_2 = E_G - \Delta_0$ and at $E_2 = E_T$, respectively, if $E_G \gg \Delta_0$. If $E_G \lesssim \Delta_0$, we use the relation $f_{\mathrm{SH}} = z(df_{\mathrm{SH}}/dz)_{z=0}$.

It is to be noted that $v/(u^2+v^2)$ in Eq. (3.26) becomes $\pi\delta(u)$ as $v \to 0+$. Actually v is finite and is at most 0.1. Thus $v/(u^2+v^2)$ shows a peak with finite width. From the definition of v the width in energy units is at most thermal energy T, comparable to the average energy of free holes. If we consider the CB and the SB, the corresponding widths, which are deduced from Eq. (3.12) to be proportional to m_C and m_S, respectively, are at most about $0.1T$. Those widths are negligible as compared to that for the HB so that we have used the free-particle Green's functions for the CB and SB in Eq. (3.1).

In order to discuss the second-order perturbation treatment of the phonon-assisted Auger process, we consider the expansion

$$G^R(l\vec{k},\omega) = G_0^R(l\vec{k},\omega) + G_0^R(l\vec{k},\omega)\Sigma^R(l\vec{k},\omega)G_0^R(l\vec{k},\omega) + \cdots \tag{3.40}$$

and retain only the first and the second terms. We use this function in Eq. (3.2). Following similar treatments below Eq. (3.2), neglecting the screening of the electron-phonon interaction, and assuming non-degenerate statistics, we obtain the minority-carrier lifetime τ_1 under this approximation as

$$\frac{1}{\tau_1} = \frac{1}{\tau_0} + \frac{70\pi^2 e^4 \hbar^3 m_H^{3/2} T^{1/2} f_{\mathrm{CH}} f_{\mathrm{SH}}}{m_0^2 m_C m_S^{1/2} \epsilon_0^2 E_G^2 (E_G - \Delta_0)^{3/2}} \times \left(A_0 + \frac{m_H}{m_S}\frac{T}{E_G - \Delta_0}B_0\right)p^2 . \tag{3.41}$$

The second term of the equation corresponds to Lochmann's result,[8] and the same approximation has been adopted. This formula is applicable only for $E_G - \Delta_0 \gg T$.

IV. RESULTS AND DISCUSSIONS

The theory developed in the previous sections is applied to p-GaAs and p-GaSb. The band parameters to be used is calculated on the basis of the $\vec{k}\cdot\vec{p}$ perturbation theory[17] using the numerical values of the interband matrix elements given by Lawaetz.[18] The calculated parameters are listed in Table IV, where m_S/m_0, f_{CH}, and f_{SH} are both

TABLE IV. Calculated band parameters.

Parameter		GaAs	GaSb
m_S/m_0		0.102	0.130
f_{CH}	77 K	5.67	9.99
f_{CH}	150 K	5.89	10.3
f_{CH}	300 K	6.00	11.2
f_{SH}	77 K	3.14	$0.0410z$
f_{SH}	150 K	3.12	$0.0812z$
f_{SH}	300 K	3.11	$0.169z$
$E_T/(E_G-\Delta_0)$	77 K	1.098	1.197
$E_T/(E_G-\Delta_0)$	150 K	1.098	0
$E_T/(E_G-\Delta_0)$	300 K	1.098	0

for the phonon-assisted Auger process and for the pure collision Auger process while $E_T/(E_G-\Delta_0)$'s are for the latter only. In order to calculate τ from Eqs. (3.25) and (3.26), computation of $S(z)$ using Weyl's *Gleichverteilung* method followed by numerical integration over z was performed. Though $v/(u^2+v^2)$ in Eq. (3.26) is a sharply peaked function around $u=0$, at most 200 combinations of (r,ϕ,ξ,η) with random values were found to yield a result which converges well for $S(z)$. The results are given in terms of the Auger coefficients C, C_1, and C_0 defined by $1/\tau=Cp^2$, $1/\tau_1=C_1p^2$ and $1/\tau_0=C_0p^2$.

In Fig. 6 we show the Auger coefficients C for p-GaAs as a function of temperature for various values of p obtained from Eq. (3.25). It is seen that C is only weakly dependent on p. In this figure is shown also the Auger coefficient C_1 calculated

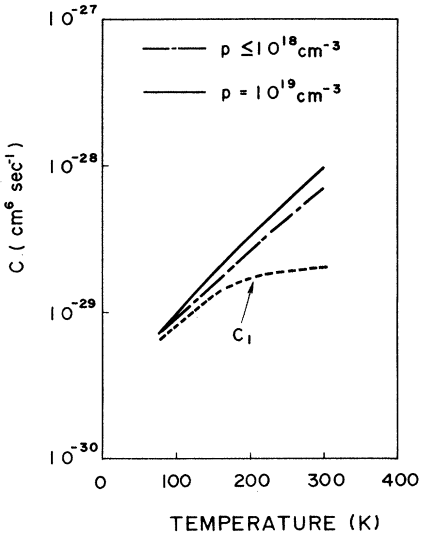

FIG. 6. Auger coefficient C for p-GaAs as a function of temperature for various hole concentrations p (—,– –). C_1 is also shown (---) using the same ordinate as for C.

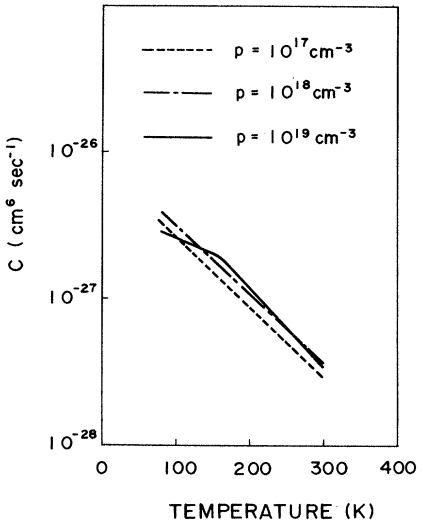

FIG. 7. Auger coefficient C for p-GaSb as a function of temperature for various hole concentrations p.

from Eq. (3.41). It is seen that though C is nearly C_1 at low temperatures, the ratio C/C_1 becomes larger and larger far beyond unity with increasing temperature. This corresponds to the fact that the condition of $E_G-\Delta_0 \gg T$ for using Eq. (3.41) is not satisfied at high temperatures.

In Fig. 7 we show the results for p-GaSb. We also find the Auger coefficients weakly dependent on p. In contrast to the case of p-GaAs C decreases with temperature mainly as a result of $E_G-\Delta_0$ changing from positive to negative value as temperature is increased. It is to be noted that Eq. (3.41) is not applicable in this case over the whole temperature range considered.

Now, comparison between C and C_0 is made. In Figs. 8 and 9 we show the ratio C/C_0. We find that in every case, including even that of the room temperature, the pure collision Auger process, i.e., C_0, is almost negligible as compared to the phonon-assisted Auger process, i.e., $C-C_0$. This is in contrast with the reported result[8] that at 300 K the phonon-assisted Auger process and the pure collision Auger process are comparable. A rapid drop of C/C_0 with increasing p occurs for p-GaAs at 77 K in the range of p exceeding 10^{18} cm^{-3}. In this range degenerate statistics are almost or perfectly applicable so that the pure collision Auger process becomes more and more important.[19]

Effect of the free-carrier screening of the electron-phonon interaction on the phonon-assisted Auger process is considered here. Hypothetically taking $\lambda=0$ for $\mathrm{Im}\Sigma^R_{1a}$ in Eq. (3.24), we calculate C. It is found that for p-GaAs the effect is almost negligible in the range $p \lesssim 10^{18}$ cm^{-3}. The effect

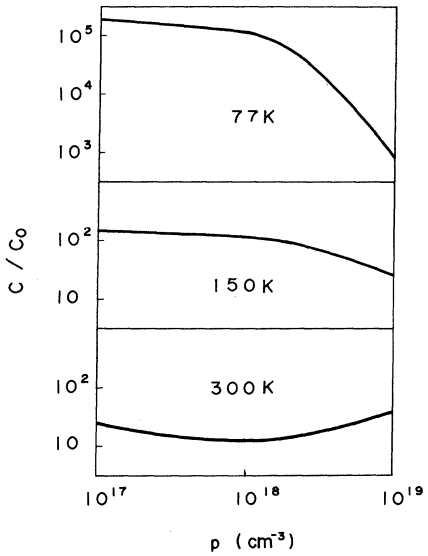

FIG. 8. Ratio C/C_0 for p-GaAs as a function of hole concentration p for various temperatures.

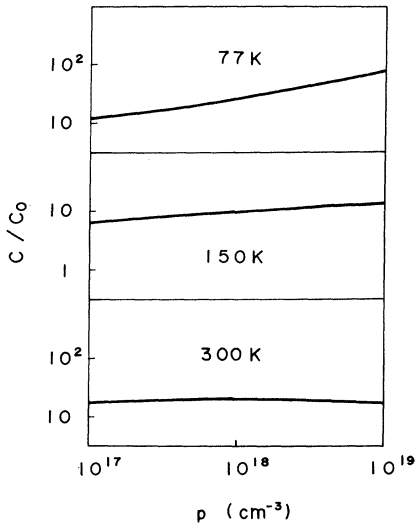

FIG. 9. Ratio C/C_0 for p-GaSb as a function of hole concentration p for various temperatures.

becomes larger with increasing p and is not negligible at $p = 10^{19}$ cm^{-3}. At this value of p the ratio $C(\lambda = 0)/C(\lambda \neq 0)$ is as large as 1.5 in the temperature range considered. For p-GaSb, on the other hand, the effect is important over the whole range of p considered. The ratio $C(\lambda \neq 0)/C(\lambda = 0)$ is as large as 2. Remarkably different features on both materials are understood from the difference that the threshold energy for the pure collision Auger process is much larger than T for p-GaAs and almost or absolutely zero for p-GaSb. For p-GaAs the phonon scattering is important mainly in reducing the threshold energy to zero: Phonons with large wave number are especially contributive to the reduction, and the screening is inefficient for those phonons. For p-GaSb, on the other hand, the phonon scattering is important only for providing a larger number of available states for the Auger transition than those for the pure collision Auger process: In this case phonons with small wave number are especially important, for which the screening is efficient and we should note that too efficient a phonon scattering reduces the Auger transition probability, as is seen from the factor $v/(u^2+v^2)$ in Eq. (3.26).

At present we have no data available to compare the present theory with experiments. We only know[20] that the radiative lifetime in p-GaAs with $p \gtrsim 10^{17}$ cm^{-3} at room temperature is several nanoseconds at the laser threshold. On the other hand, the calculated Auger lifetime is below 10 nsec in the range $p \gtrsim 10^{18}$ cm^{-3} and decreases nearly in proportion to p^{-2}. Thus in analyzing operations of light-emitting diodes and laser diodes it will be important to take into account the Auger recombination.

In this paper we have not included the electron-impurity interaction. This has been shown in the literature[11] to be important especially in the range $p \gtrsim 10^{19}$ cm^{-3}. In the literature, however, effects of the phonon scattering and the impurity scattering have been considered separately. Investigation of combined effects of both scatterings is necessary especially in the range $p > 10^{18}$ cm^{-3} and will be considered in the future.

ACKNOWLEDGMENT

The author wishes to express his appreciation to Dr. I. Teramoto and Dr. H. Mizuno for their constant encouragement.

[1]For review articles see: P. T. Landsberg, Phys. Status Solidi A 41, 457 (1970); A. Haug, in *Festkörperprobleme, Advances in Solid State Physics*, edited by O. Madelung (Pergamon, Braunschweig, 1972), Vol. XII, p. 411; R. Conradt, in *Festkörperprobleme, Advances in Solid State Physics*, Vol. XII, p. 449; P. T. Landsberg and M. J. Adams, J. Lumin. 7, 3 (1973).

[2]M. Takeshima, J. Appl. Phys. 46, 3082 (1975).
[3]L. Huldt, Phys. Status Solidi A 8, 173 (1971).
[4]L. Huldt, Phys. Status Solidi A 24, 221 (1974).
[5]D. Hill and P. T. Landsberg, Proc. R. Soc. London Ser. A 347, 547 (1976).
[6]G. Benz and R. Conradt, Phys. Rev. B 16, 843 (1977).
[7]L. Huldt, Phys. Status Solidi A 33, 607 (1976).
[8]W. Lochmann, Phys. Status Solidi A 40, 285 (1977).
[9]W. Lochmann, Phys. Status Solidi A 42, 181 (1977).
[10]W. Lochmann, Phys. Status Solidi A 45, 423 (1978).
[11]Masumi Takeshima, Phys. Rev. B 23, 771 (1981).
[12]A. A. Abrikosov, L. P. Gor'kov, and L. E. Dzyaloshinskii, *Methods of Quantum Field Theory in Statistical Physics* (Prentice-Hall, Englewood Cliffs, 1965).
[13]S. Doniach and E. H. Sondheimer, *Green's Function for Solid State Physicists* (Benjamin, Massachusetts, 1974), Chap. 5.
[14]V. L. Bonch-Bruevich and S. L. Tyablikov, *The Green Function Method in Statistical Mechanics* (North-Holland, Amsterdam, 1962), Chaps. 1 and 2.
[15]A. R. Beatie and G. Smith, Phys. Status Solidi A 19, 577 (1967).
[16]A. R. Beatie and P. T. Landsberg, Proc. R. Soc. London Ser. A 249, 16 (1959).
[17]Semiconductor and Semimetals, edited by R. K. Willardson and A. C. Beer (Academic, New York, 1966) Vol. 1, Chap. 3.
[18]P. Lawaetz, Phys. Rev. B 4, 3460 (1971).
[19]K. H. Zschauer, Solid State Commun. 7, 1709 (1969).
[20]C. J. Hwang and J. C. Dyment, J. Appl. Phys. 44, 3240 (1973).